Emerin regulation of nuclear stiffness is required for the amoeboid migration of cancer cells in confining environments

Lavenus, Sandrine B., Vosatka, Karl W., Ullo, Maria F., and Logue, Jeremy S.*

Department of Regenerative and Cancer Cell Biology, Albany Medical College, 47 New Scotland Ave, Albany, NY 12208, USA

*Corresponding author

loguej@mail.amc.edu

Running head: Emerin regulates the migration of confined cells

Abstract

Through the process of regulating cell deformability in confined environments, the nucleus has emerged as a major regulator of cell migration. Here, we demonstrate that nuclear stiffness regulates the confined (leader bleb-based) migration of cancer cells. Using high-resolution imaging, we demonstrate that modifying the level of the Inner Nuclear Membrane (INM) protein, emerin, will inhibit Leader Bleb-Based Migration (LBBM). In line with the notion that nuclear stiffness regulates LBBM, stiffness measurements indicate that nuclei are softest at endogenous levels of emerin. Emerin has been found to be phosphorylated by Src in response to force, increasing nuclear stiffness. Accordingly, we found LBBM to be insensitive to increasing levels of emerin (Y74F/Y95F). Using a biosensor, Src activity is found to negatively correlate with cell confinement. Thus, our data are consistent with a model in which low Src activity maintains a soft nucleus and promotes the confined (leader bleb-based) migration of cancer cells.

Keywords: cancer, metastasis, cell migration, cytoskeleton, nucleus, nuclear envelope, emerin, Src, mechanotransduction

Introduction

Cell migration is essential to maintain homeostasis within normal tissues, whereas uncontrolled cell migration is often a hallmark of disease. In cancer, metastasis requires that cells migrate away from the primary tumor. Accordingly, elucidating the molecular mechanisms required by motile cancer cells may provide therapeutic targets for the abatement or prevention of metastasis[1]. However, the discovery that cancer cells may use multiple migration modes, including mesenchymal, collective, lobopodial, osmotic engine, and amoeboid has made this effort challenging[2-5]. Therefore, studies that aim to identify broadly (i.e., effecting multiple modes) important factors may be of particularly high value. As motile cancer cells must traverse the confines of tissues, regulators of cancer cell stiffness are likely to affect all migration modes. In line with this notion, the deformation of the cell nucleus has been shown to be a rate limiting step to migration within tissues[6]. Although the importance of the lamin intermediate filaments (e.g., Lamin A/C) is clear, the contribution of Inner Nuclear Membrane (INM) proteins (which may regulate nuclear stiffness in response to force) in regulating cell migration is poorly understood.

In order to travel to distant metastatic sites, cancer cells have been shown to utilize a variety of migration modes. One such mode, referred to as fast amoeboid migration[7], requires what we termed a 'leader bleb'[8]. Like other blebs, leader blebs are an intracellular pressure driven protrusion of the plasma membrane[9]. However, leader blebs are unique in that they are not immediately retracted following cortical actomyosin recruitment. Instead, these are large and stable blebs with flowing cortical actomyosin[7, 8, 10]. Remarkably, it is this continuous flow of cortical actomyosin that drives Leader Bleb-Based Migration (LBBM). In contrast to mesenchymal cells that require substrate adhesion, only non-specific friction between leader blebs and the environment is required for cell movement[11]. However, this type of motility appears to be largely restricted to transformed cells[7]. Furthermore, this phenotypic transition

has been found to be promoted by cell confinement[7, 8, 10, 11]. Although compressing the cell (i.e., confinement) may be sufficient to pressurize the cytoplasm, recent studies have suggested that cells adapt to confinement by upregulating actomyosin contractility[12, 13]. Because of this dependence on confinement, rapid LBBM is likely to require the precise tuning of cell stiffness.

As it is the largest organelle, the deformability of the cell nucleus is a major regulator of confined migration[14]. Professionally migrating cells, such as immune cells, have soft nuclei as a result of having low levels of Lamin A/C[15]. Similarly, low Lamin A/C levels have been found in motile cancer cells[16]. However, the role of lamin-associated factors in confined migration, which can regulate nuclear stiffness in response to force, is not well understood. Using magnetic tweezers and isolated nuclei, the LEM (LAP2, emerin, MAN1) domain containing protein, emerin, was identified as a candidate factor regulating the response of nuclei to force[17]. It was found that isolated nuclei were stiffer in the absence of emerin, while isolated nuclei with emerin were softer. However, upon repeated force application, isolated nuclei became progressively stiffer in an emerin-dependent manner. Moreover, this effect was found to require the tyrosine phosphorylation of emerin (Y74/95) by Src[17, 18]. Thus, emerin is required for nuclear adaptation to force.

Here, our results suggest that in cancer cells (which have been derived from distant metastases) the concentration of emerin has been precisely selected, as either RNAi or Over-Expression (OE) of emerin suppresses confined (leader bleb-based) migration. Additionally, isolated nuclei were softest at endogenous levels of emerin. However, cells were found to be insensitive to increasing levels of a non-phosphorylatable (Y74F/Y95F) version of emerin. Thus, confined (leader bleb-based) migration is found to require emerin regulation of nuclear stiffness.

Results

Because the invasive front of melanoma tumors has been previously shown to be enriched with amoeboid cells[19-21], we chose to use human melanoma A375-M2 cells for studying the role of nuclear stiffness in the regulation of LBBM. For live high-resolution imaging of fast amoeboid cells, we used our previously described Polydimethylsiloxane (PDMS) slab-based approach[22]. This method involves placing cells underneath a BSA-coated (1 mg/mL) slab of PDMS, which is supported above cover glass at a defined height by micron-sized beads (~3 μm). Using this simplified system, we can reproducibly subject cells to a force (i.e., compression) commonly found in tissues, promoting the switch to LBBM. Upon transient transfection of EGFP alone, time-lapse imaging reveals that cells either form leader blebs and are mobile (leader mobile; LM) (44.6%), form leader blebs and are non-mobile (leader non-mobile; LNM) (26.4%), or do not form a leader bleb (no leader; NL) (29.1%) (Fig. 1A & Movies S1-3). We were curious to know why a significant fraction of these cells form leader blebs but are non-mobile (LNM; 26.4%); therefore, we transiently transfected cells with H2B-mEmerald and F-tractin-FusionRed to mark nuclei and F-actin, respectively, and performed time-lapse imaging. Similar to the mobile fraction, cells formed a single large leader bleb but were unable to move (Fig. 1A & Movies S1-2). Moreover, we found that the nucleus undergoes dramatic shape changes and can move into leader blebs (Fig. 1B-C). Accordingly, we set out to determine if nuclear stiffness regulates LBBM. As a first approach, we evaluated the effect of Lamin A/C on LBBM. Upon over-expressing Lamin A/C-mEmerald, the nucleus was found to adopt a more rounded shape after comparing nuclear aspect ratios (Fig. 1B). Additionally, the number of leader blebs containing the cell nucleus was reduced by ~50% (Fig. 1C). The number of leader mobile cells was also reduced by ~50%, whereas the speed of leader mobile cells was unchanged in Lamin A/C over-expressing cells (Fig. 1D-E). Consistent with our analysis of cell fractions, an analysis of all cells revealed a statistically significant reduction in instantaneous speed (Fig. S4B). Although Lamin A/C RNAi led to less round nuclei and more leader blebs containing the nucleus, leader bleb area, the number of leader mobile cells, and the instantaneous speed of

these and of all cells was not significantly different from control (Fig. S1A-G & S4A). Because cancer cells are known to have low levels of Lamin A/C, it may not be surprising that further decreasing the level of Lamin A/C does not have a more profound effect[16]. Interestingly, while the fraction of leader mobile cells was decreased upon over-expressing Lamin A/C, the fraction of leader non-mobile cells was unchanged (Fig. 1D). Instead, the fraction of cells without leader blebs, i.e., do not form a single large bleb, was nearly doubled in cells over-expressing Lamin A/C (Fig. 1D). Accordingly, cells over-expressing Lamin A/C formed smaller blebs (Fig. 1F). Thus, these results suggest that nuclear stiffness is a major regulator of LBBM.

The Inner Nuclear Membrane (INM) protein, emerin, has been identified as a candidate factor regulating the response of nuclei to force[17]. Similar to Lamin A/C, we wondered if emerin through the dynamic regulation of nuclear stiffness is important for confined migration. In confined cells, EGFP-emerin was primarily localized to the nuclear envelope (Fig. 2A & Movie S4). Moreover, this localization was maintained throughout time-lapse imaging. Interestingly, emerin RNAi and over-expression led to similar phenotypes. More specifically, comparing nuclear aspect ratios showed that emerin RNAi and over-expressing cells have more rounded nuclei, whereas the number of leader blebs containing the nucleus was decreased (Fig. 2B-C). Although the instantaneous speed of leader mobile cells was similar, the number of leader mobile cells was decreased by over 50% (Fig. 2D-E). Furthermore, these results paralleled an analysis of instantaneous speeds for all cells (Fig. S4A-B). For emerin RNAi, leader mobile (LM) cells were redistributed to the leader non-mobile (LNM) and no leader (NL) fractions (Fig. 2D, left). In contrast, emerin over-expression only increased the no leader (NL) fraction (Fig. 2D, right). In agreement with this result, bleb area was significantly decreased only in emerin over-expressing cells (Fig. 2F). In order to assess the general requirement for emerin in confined migration, we subjected cells to transmigration assays. Using filters with 8 μm pores, we observed an over 50% decrease in transmigration after emerin RNAi (Fig. 2G, left). In

contrast, depleting cells of emerin had no effect on transmigration through 12 µm filters (Fig. 2G, right). Thus, confined migration is tightly regulated by the level of emerin.

In order to more precisely determine the role of emerin in regulating confined (leader bleb-based) migration, we next turned to a previously described gel sandwich assay for measuring cell stiffnesses[7, 23]. Briefly, this assay involves placing cells between two polyacrylamide gels of known stiffness (1 kPa; Fig. 3A). The ratio of the cell height to the diameter (i.e., deformation) is used to define stiffness (Fig. 3A). After emerin RNAi, cell stiffness increased by ~15%, whereas an over 25% decrease in cell stiffness was observed after Lamin A/C RNAi (Fig. 3B). When compared to EGFP alone, the stiffness of cells over-expressing emerin or Lamin A/C was not significantly different (Fig. 3C). As a first approach to measuring nuclear stiffness, we subjected cells to Latrunculin-A (Lat-A; 500 nM) to depolymerize actin. In control (non-targeting) cells, stiffness was reduced by over 60% by Lat-A treatment (Fig. 3D). Using this approach, emerin RNAi cells were found to be ~65% stiffer, whereas the stiffness of Lamin A/C RNAi cells was not significantly different from control (non-targeting; Fig. 3D). In cells treated with Lat-A, stiffness was reduced by ~45% after over-expressing emerin (Fig. 3E). Lamin A/C over-expression increased stiffness by ~55% (Fig. 3E). Next, this assay was combined with cell fractionation for measuring the stiffness of isolated nuclei. Using this approach, isolated nuclei were 20% stiffer after over-expressing Lamin A/C (Fig. 3F). In contrast to in cells treated with Lat-A, we found that over-expressing emerin increased the stiffness of isolated nuclei by ~25% (Fig. 3F). Thus, in cells over-expressing emerin, F-actin appears to be required for nuclear stiffening.

Although predominantly localized to the Inner Nuclear Membrane (INM), emerin can also be found within the Outer Nuclear Membrane (ONM) and contiguous ER[24]. Accordingly, we wondered if by over-expressing emerin the level of this protein was increased within the ONM and ER, controlling nuclear stiffness. To address this possibility, we utilized a previously

described frame shift mutation, Phe240His-FS, located near the transmembrane domain for retaining emerin within the ONM and ER (ΔINM; Fig. S2A)[25]. In confined cells, emerin ΔINM was enriched within the ONM/ER (Fig. S2B). Interestingly, cell stiffness was increased by over 35% after over-expressing emerin ΔINM (Fig. 3C). In contrast, the stiffness of cells treated with Lat-A or isolated nuclei was unchanged after over-expressing emerin ΔINM (Fig. 3E-F). Additionally, nuclear aspect ratio and the number of leader blebs containing the nucleus was not significantly different from control (EGFP alone; Fig. S2C-D). However, the number of leader mobile (LM) cells and leader bleb area were reduced relative to control (EGFP alone; Fig. S2E-G & S4B). These data suggest that emerin localized within the INM and not ONM and ER regulates nuclear stiffness. However, our data also show that the number of leader mobile and leader bleb area are reduced relative to control (EGFP alone); therefore, emerin ΔINM may take on additional (unknown) functions in the cytoplasm.

As emerin has actin pointed-end capping activity (inhibiting de-polymerization), emerin at the ONM and ER may affect LBBM through the regulation of actomyosin dynamics. Accordingly, we used a previously described point mutant, Q133H, to evaluate the role of emerin actin pointed-end capping activity in LBBM[26]. Actin pointed-end capping activity was found to not be required for the localization of emerin at the nuclear envelope, as demonstrated by live high-resolution imaging (Fig. S3A). Upon over-expressing emerin Q133H, cell stiffness was increased by ~10% (Fig. 3C). In cells treated with Lat-A or isolated nuclei, stiffness was not significantly different from control (EGFP alone; Fig. 3E-F). Consistent with the notion that nuclear stiffness regulates LBBM, nuclear aspect ratio, the number of leader blebs containing the nucleus, the number of leader mobile (LM) cells, and leader bleb area were unaffected by the over-expression of emerin Q133H (relative to EGFP alone; Fig. S3B-F & S4B). Additionally, the total level of F-actin was unchanged in emerin RNAi and over-expressing (emerin WT, ΔINM, and Q133H) cells, as demonstrated by flow cytometry analysis (Fig. S5A-B). As

opposed to regulating actomyosin dynamics in the cytoplasm, these data suggest that emerin actin pointed-end capping activity is important for nuclear stiffening.

It has been demonstrated that emerin is phosphorylated by Src in response to force, increasing nuclear stiffness[17, 18]. Therefore, we wondered if cells would be agnostic to increasing levels of a non-phosphorylatable (Y74F/Y95F) version of emerin. Relative to emerin WT, we found that the effect on nuclear aspect ratio, the number of leader blebs containing the nucleus, and the number of leader mobile (LM) cells was reduced when over-expressing emerin Y74F/Y95F (Fig. 4B-E & Movie S5). Consistent with these results, the stiffness of isolated nuclei was unaffected by the over-expression of emerin Y74F/Y95F (Fig. 4F-G). Moreover, leader bleb area was not significantly different from control (EGFP alone; Fig. 4H). Using the Src family kinase inhibitor, Dasatinib, we confirmed that the activity of this kinase is important for regulating the stiffness of isolated nuclei (Fig. 5A). As these data would suggest that high Src activity would inhibit confined migration, we next set out to determine the level of Src activity in unconfined vs. confined cells. For measuring Src activity in confined cells, we used a previously described FRET biosensor made using ECFP (donor), an SH2 domain, linker, Src substrate peptide, YPet (acceptor), and a membrane anchor[27]. To quantitatively compare Src activity across many cells, FRET efficiencies were calculated after acceptor photobleaching in unconfined vs. confined cells[28]. In cells plated on uncoated cover glass, we calculated an average FRET efficiency of 17.29% (+/- 0.0724; SD) (Fig. 5B-C). Interestingly, in cells confined under PDMS slabs, we calculated an average FRET efficiency of 8.457% (+/- 0.03224; SD) (Fig. 5B-C). Therefore, our data supports a model in which Src activity is inhibited in confined (non-adherent) cells and through maintaining a soft nucleus, promotes confined (leader bleb-based) migration.

Discussion

In the present study, we have determined that the stiffness of the cell nucleus is a major regulator of confined (leader bleb-based) migration. By manipulating the level of Lamin A/C, nuclear stiffening was shown to decrease the number of leader mobile cells. In addition to changes in nuclear shape and position, the area of leader blebs was reduced after over-expressing Lamin A/C. This suggests that a stiff nucleus may limit the compressibility of the cell body, reducing leader bleb area. Similarly, we reported that high levels of Vimentin (which is also localized to the cell body) will through the regulation of cell mechanics limit leader bleb area and migration[23]. After confirming our initial hypothesis, which was that nuclear stiffness is important for LBBM, we next set out to determine the precise role of mechanosensitive (Lamin associated) factors in confined (leader bleb-based) migration.

The INM localized protein, emerin, was found to be phosphorylated by Src in response to force, increasing nuclear stiffness[17, 18]. Here, we describe for the first time that confined (leader bleb-based) migration depends on a precise level of emerin. As demonstrated by RNAi and over-expression, nuclei were found to be softest at endogenous levels of emerin (Fig. 5D). Accordingly, LBBM is promoted by the endogenous level of emerin. In light of these results, we speculate that the level of emerin in cancer cells has undergone selection, increasing metastasis. Moreover, this requirement does not appear to be specific for LBBM, as transmigration through 8 and not 12 µM pores is inhibited by emerin RNAi. As a first approach for measuring nuclear stiffness, we combined the gel sandwich assay with Lat-A treatment (depolymerizing actin). After emerin RNAi, we observed a large increase in stiffness, whereas (surprisingly) emerin over-expression decreased stiffness. Using isolated nuclei, which does not require the removal of F-actin, emerin over-expression increased nuclear stiffness (the effect of emerin RNAi remained the same). Thus, our data suggest F-actin is required for emerin function.

Using a frame shift mutant (Phe240His-FS) for retaining emerin in the ONM/ER[25], we could confirm that nuclear stiffening requires that emerin be localized to the INM. However, using the gel sandwich assay on untreated cells, we found that the over-expression of emerin ΔINM led to a large increase in stiffness. Moreover, the number of leader mobile and leader bleb area were reduced relative to control (EGFP alone). These results suggest that emerin in the ONM/ER may take on additional (unknown) functions, decreasing LBBM. Interestingly, it has been shown that the localization of emerin can shift from the INM to ONM/ER in response to force, controlling actomyosin dynamics in the cytoplasm[24, 29]. Although we were unable to detect a significant difference in the level of emerin in the ONM/ER in unconfined vs. confined cells, we wondered if emerin actin pointed-end capping activity is important for LBBM. Thus, we used a previously described point mutant, Q133H, for evaluating the role of emerin actin pointed-end capping activity in confined cells[26]. Surprisingly, the over-expression of emerin Q133H increased LBBM (relative to emerin WT). In line with the notion that nuclear stiffness regulates LBBM, the over-expression of emerin Q133H decreased the stiffness of isolated nuclei (relative to emerin WT). Therefore, we speculate that through stabilizing actin at the INM that pointed-end capping by emerin is important for nuclear stiffening.

Emerin has been reported to be phosphorylated by Src in response to force, increasing nuclear stiffness[17, 18]. Accordingly, we set out to determine how over-expressing a non-phosphorylatable version of emerin (Y74F/Y95F) would affect confined (leader bleb-based) migration. In cells over-expressing emerin Y74F/Y95F, we found the number of leader mobile cells and leader bleb area to be increased (relative to emerin WT). Additionally, isolated nuclei were softer when over-expressing emerin Y74F/Y95F (relative to emerin WT). In light of these data, high Src activity should inhibit confined migration; therefore, we determined the level of Src activity in unconfined vs. confined cells. Strikingly, we found Src activity to be significantly lower in confined (non-adherent) cells, as determined by a FRET biosensor. Thus, our data

suggest that over-expressing emerin will make nuclei hypersensitive to Src (Fig. 5C-D). This effect is unlikely to be due to differences in the level of adhesion, as unconfined cells were freshly plated on cover glass. Alternatively, we speculate that low Src activity is a consequence of the dynamic cortical actin network in confined cells. In support of this notion, receptor tyrosine kinase activity is enhanced by interactions with cortical actin-plasma membrane linkers (e.g., Ezrin)[30]. These data are also consistent with previous work from our lab, which demonstrated that the introduction of a constitutively active version of Src reduces LBBM[3, 4]. In contrast to the better known mechanisms of mechanotransduction in adherent cells (which often involve Src), cells may use different mechanisms for sensing confinement[31]. This idea is supported by recent evidence that the INM unfolds and activates a cytosolic Phospholipase A2 (cPLA2)-dependent mechanotransduction pathway in confined cells, increasing actomyosin contractility[12, 13].

In conclusion, we find that emerin regulation of nuclear stiffness is required for the confined (leader bleb-based) migration of cancer cells. Future work will aim to address the molecular mechanism by which emerin regulates nuclear stiffness and whether (small molecule) modulators of nuclear stiffness can be used to inhibit metastasis.

SUPPLEMENTAL INFORMATION

Supplemental information includes 5 figures and 5 movies and can be found with this article online.

METHODS

Cell culture

A375-M2 cells (CRL-3223) were obtained from the American Type Culture Collection (ATCC; Manassas, VA). Cells were cultured in high-glucose DMEM supplemented with 10% FBS (cat no. 12106C; Sigma Aldrich, St. Louis, MO), GlutaMAX (Thermo Fisher Scientific, Carlsbad, CA),

antibiotic-antimycotic (Thermo Fisher Scientific), and 20 mM HEPES at pH 7.4 for up to 30 passages. Cells were plated at a density of 750,000 cells per well in a 6-well plate the day of transfection.

Pharmacological treatments

Latrunculin-A (cat no. 3973) and Dasatinib (cat no. 6793) were purchased from Tocris Bioscience (Bristol, UK). DMSO (Sigma Aldrich) was used to make 1 mM and 0.5 mM stock solutions of Latrunculin-A and Dasatinib, respectively. Prior to cell stiffness measurements, polyacrylamide gels were incubated for 30 min in buffer S (20 mM HEPES at pH 7.8, 25 mM KCl, 5 mM $MgCl_2$, 0.25 M sucrose, and 1 mM ATP) with DMSO, Latrunculin-A, or Dasatinib.

Plasmids

F-tractin-FusionRed has been previously described[8]. H2B-FusionRed was purchased from Evrogen (Russia). mEmerald-Lamin A-C-18 (Addgene plasmid no. 54138) and mEmerald-Nucleus-7 (Addgene plasmid no. 54206) were gifts from Michael Davidson (Florida State University). Emerin pEGFP-N2 (588; Addgene plasmid no. 61985) and Emerin pEGFP-C1 (637; Addgene plasmid no. 61993) were gifts from Eric Schirmer (University of Edinburgh). Kras-Src FRET biosensor (Addgene plasmid no. 78302) was a gift from Yingxiao Wang (University of Illinois). 1 µg of plasmid was used to transfect 750,000 cells in each well of a 6-well plate using Lipofectamine 2000 (5 µL; Thermo Fisher Scientific) in OptiMEM (400 µL; Thermo Fisher Scientific). After 20 min at room temperature, plasmid in Lipofectamine 2000/OptiMEM was then incubated with cells in complete media (2 mL) overnight.

Mutagenesis

Mutants and RNAi resistant forms of emerin and Lamin A/C were generated using the QuikChange II XL Site-Directed Mutagenesis Kit (Agilent Technologies; Santa Clara, CA) according to the manufacture's protocol. The following primers were used for PCR:

Phe240His-FS (ΔINM)		Forward	GTGATCGTCCTCCATTTACCACTTC
		Reverse	GAAGTGGTAAATGGAGGACGATCAC
Q133H		Forward	GCTTTCCATCACCATGTGCATGATGACG
		Reverse	CGUCAUCAUGCACUGGUGAUGAUGGAAAGC
Y74F/Y95F	Y74F	Forward	GGGATGCAGATATGTTTGATCTTCCCAAGAAAGAGGA
		Reverse	TCCTCTTTCTTGGGAAGATCAAACATATCTGCATCCC
	Y95F	Forward	GGCTACAATGACGACTACTTTGAAGAGAGCTACTTC
		Reverse	GAAGTAGCTCTCTTCAAAGTAGTCGTCATTGTAGCC
RNAi resistant	Emerin	Forward	CTCCCTGGACCTGTCTTATTATCCTACTTCC
		Reverse	GGAAGUAGGAUAAUAAGACAGGUCCAGGGAG
	Lamin A/C	Forward	TACCAAGAAGGAGGGCGACCTGATAGCTGCT
		Reverse	AGCAGCTATCAGGTCGCCCTCCTTCTTGGTA

RNAi resistant emerin yields a single (silent; C->T) mutation centrally located within the LNA target sequence (GACCTGTCCTATTATCCTA). RNAi resistant Lamin A/C yields a single (silent; T->C) mutation centrally located within the LNA target sequence (GAAGGAGGGTGACCTGATA). All clones were verified by sequencing using a commercially available resource (Genewiz, South Plainfield, NJ).

LNAs

Non-targeting (cat no. 4390844), Lamin A/C (cat no. 4390824; s8221), and emerin (cat no. 4392420; s225840) Locked Nucleic Acids (LNAs) were purchased from Thermo Fisher Scientific. All LNA transfections were performed using RNAiMAX (5 µL; Thermo Fisher Scientific) and OptiMEM (400 µL; Thermo Fisher Scientific). Briefly, cells were trypsinized and seeded in 6-well plates at 750,000 cells per well in complete media. After cells adhered (~1 hr), LNAs in RNAiMAX/OptiMEM were added to cells in complete media (2 mL) at a final concentration of 50 nM. Cells were incubated with LNAs for as long as 5 days.

Western blotting

Whole-cell lysates were prepared by scraping cells into ice cold RIPA buffer (50 mM HEPES pH 7.4,150 mM NaCl, 5 mM EDTA, 0.1% SDS, 0.5% deoxycholate, and 1% Triton X-100) containing protease and phosphatase inhibitors (Roche, Switzerland). Before loading onto 4–12% NuPAGE Bis-Tris gradient gels (Thermo Fisher Scientific), DNA was sheared by sonication and samples were boiled for 10 min in loading buffer. Following SDS-PAGE, proteins in gels were transferred to nitrocellulose membranes and subsequently immobilized by air drying overnight. After blocking in Tris-Buffered Saline containing 0.1% Tween 20 (TBS-T) and 1% BSA, primary antibodies against Lamin A/C (cat no. 2032; Cell Signaling Technology) or emerin (cat no. 30853; Cell Signaling Technology) were incubated with membranes overnight at 4 °C. Bands were then resolved with Horse Radish Peroxidase (HRP) conjugated secondary antibodies and a C-Digit imager (LI-COR Biosciences, Lincoln, NE). GAPDH (cat no. 97166; Cell Signaling Technology) was used to confirm equal loading.

Microscopy

Live high-resolution imaging was performed using a General Electric (Boston, MA) DeltaVision Elite imaging system mounted on an Olympus (Japan) IX71 stand with a computerized stage, environment chamber (heat, CO_2, and humidifier), ultrafast solid-state illumination with excitation/emission filter sets for DAPI, CFP, GFP, YFP, and Cy5, critical illumination, Olympus PlanApo N 60X/1.42 NA DIC (oil) objective, Photometrics (Tucson, AZ) CoolSNAP HQ2 camera, proprietary constrained iterative deconvolution, and vibration isolation table.

Confinement

This protocol has been described in detail elsewhere[22]. Briefly, PDMS (Dow Corning 184 SYLGARD) was purchased from Krayden (Westminster, CO). 2 mL was cured overnight at 37

°C in each well of a 6-well glass bottom plate (Cellvis, Mountain View, CA). Using a biopsy punch (cat no. 504535; World Precision Instruments, Sarasota, FL), an 8 mm hole was cut and 3 mL of serum free media containing 1% BSA was added to each well and incubated overnight at 37 °C. After removing the serum free media containing 1% BSA, 200 µL of complete media containing trypsinized cells (250,000 to 1 million) and 2 µL of beads (3.11 µm; Bangs Laboratories, Fishers, IN) were then pipetted into the round opening. The vacuum created by briefly lifting one side of the hole with a 1 mL pipette tip was used to move cells and beads underneath the PDMS. Finally, 3 mL of complete media was added to each well and cells were recovered for ~60 min before imaging.

Leader blebs containing the cell nucleus

A thematic analysis of leader blebs and the nucleus was done for every cell by eye. If the nucleus moved into the leader bleb from the cell body and remained there for at least 3 consecutive frames, the cell was classified as having a 'leader bleb containing the nucleus'.

Classification of leader mobile (LM), leader non-mobile (LNM), and no leader (NL) cells

For classification, freshly confined cells were imaged every 8 min for 5 hr. Cells were classified by eye as either leader mobile (LM; cells that undergo fast directionally persistent leader bleb-based migration), leader non-mobile (LNM; cells with a leader bleb that persists for at least 5 frames but do not move), or no leader (NL; cells that undergo slow directionally non-persistent bleb-based migration).

Instantaneous speed

Cells were tracked manually using the Fiji (https://fiji.sc/) plugin, MTrackJ, developed by Meijering and colleagues[32, 33]. Instantaneous speeds from manual tracking was determined using the Microsoft Excel plugin, DiPer, developed by Gorelik and colleagues[32, 33]. For

minimizing positional error, cells were tracked every 8 min for 5 hr. Brightfield imaging was used to confirm that beads were not obstructing the path of a cell.

Leader bleb area

For leader bleb area, freshly confined cells were imaged every 8 min for 5 hr and cells were traced from high-resolution images with the free-hand circle tool in Fiji (https://fiji.sc/). From every frame, the percent of total cell area for leader blebs was calculated in Microsoft Excel (Redmond, WA) as the measured leader bleb area divided by the total cell area for the same frame. Measurements were then combined to generate an average for each cell.

Cell stiffness assay

The previously described gel sandwich assay was used with minor modifications[7]. 6-well glass bottom plates (Cellvis) and 18 mm coverslips were activated using 3-aminopropyltrimethoxysilane (Sigma Aldrich) for 5 min and then for 30 min with 0.5% glutaraldehyde (Electron Microscopy Sciences, Hatfield, PA) in PBS. 1 kPa polyacrylamide gels were made using 2 µL of blue fluorescent beads (200 nm; ThermoFisher), 18.8 µL of 40% acrylamide solution (cat no. 161-0140; Bio-Rad, Hercules, CA), and 12.5 µL of bis-acrylamide (cat no. 161-0142; Bio-Rad) in 250 µL of PBS. Finally, 2.5 µL of Ammonium Persulfate (APS; 10% in water) and 0.5 µL of Tetramethylethylenediamine (TMED) was added before spreading 9 µL drops onto treated glass under coverslips. After polymerizing for 40 min, the coverslip was lifted in PBS, extensively rinsed and incubated overnight in PBS. Before each experiment, the gel attached to the coverslip was placed on a 14 mm diameter, 2 cm high PDMS column for applying a slight pressure to the coverslip with its own weight. Then, both gels were incubated for 30 min in media (cells) or buffer S (isolated nuclei) before plates were seeded. After the bottom gels in plates was placed on the microscope stage, the PDMS column with the top gel was placed on top of the cells seeded on the bottom gels, confining cells between the two gels

(Fig. 2G). After 1 hr of adaptation, the height of cells was determined with beads by measuring the distance between gels, whereas the cell diameter was measured using a far-red plasma membrane dye (cat no. C10046; ThermoFisher). Stiffness was defined as the height (*h*) divided by the diameter (*d*). If drugs were used, gels were first incubated with drug in media for 30 min before an experiment.

Nucleus isolation

The protocol for isolating nuclei has been previously described[17]. 24 hr prior to nucleus isolation, 750,000 cells per well in a 6-well plate were transfected using Lipofectamine 2000 (5 µL; Thermo Fisher Scientific) as needed. Cells were lysed in 1 mL of hypotonic buffer (10 mM HEPES, 1 mM KCl, 1 mM $MgCl_2$, 0.5 mM dithiothreitol, and protease inhibitors) for 10 min on ice. After cell fragments were detached using a scraper, samples were homogenized using 50 strokes of a tight-fitting Dounce homogenizer and then centrifuged at 700 x g for 10 min at 4 °C. Pellets were then washed in hypotonic buffer and centrifuged again. The nuclear pellet was then suspended in buffer S (20 mM HEPES at pH 7.8, 25 mM KCl, 5 mM $MgCl_2$, 0.25 M sucrose, and 1 mM ATP) and then stained with a far-red fluorescent membrane dye (cat no. C10046; Thermo Fisher Scientific). Prior to the cell stiffness assay, the number and purity of nuclei was assessed by size was determined using an automated cell counter (TC20; Bio-Rad, Hercules, CA).

Transmigration

Transmigration assays were performed using polycarbonate filters with 8 or 12 µm pores (Corning; Corning, NY). Prior to the assays, polycarbonate filters were coated with fibronectin (10 µg/mL; Millipore) then air dried for 1 hr. 100,000 cells in serum free media were seeded in the top chamber while the bottom chamber contained media with 20% FBS to attract cells. After 24 hr, cells from the bottom of the filter were trypsinized and counted using an automated cell

counter (TC20; Bio-Rad). Transmigration was then calculated as the ratio of cells on the bottom of the filter vs. the total.

Src biosensor

FRET efficiencies in unconfined vs. confined cells transfected with the Kras-Src FRET biosensor (Addgene plasmid no. 78302; gift from Yingxiao Wang) were calculated using the acceptor photobleaching method[28].

Flow cytometry

For measuring F-actin, trypsinized cells in FACS buffer (PBS with 1% BSA) were fixed using 4% paraformaldehyde (cat no. 15710; Electron Microscopy Sciences) for 20 min at room temperature. After washing, cells were stained with Alexa Fluor 647 conjugated phalloidin (cat no. A22287; Thermo Fisher Scientific) and DAPI (Sigma Aldrich) overnight at 4 °C. Data were acquired on a FACSCalibur (BD Biosciences, Franklin Lakes, NJ) flow cytometer. Median Fluorescence Intensities (MFIs) were determined using FlowJo (Ashland, OR) software. A detailed description of the flow gating strategy is shown in figure S5B.

Statistics

All sample sizes were empirically determined based on saturation. As noted in each figure legend, statistical significance was determined by either a two-tailed Student's t-test, multiple-comparison test post-hoc, or Chi-squared test. Normality was determined by a D'Agostino & Pearson test in GraphPad Prism. * - $p \leq 0.05$, ** - $p \leq 0.01$, *** - $p \leq 0.001$, and **** - $p \leq 0.0001$

Data availability

The data that support the findings of this study are available from the corresponding author, J.S.L., upon reasonable request.

ACKNOWLEDGEMENTS

We thank members of the Logue Lab for insightful discussions and critical reading of this manuscript. We would also like to thank the administrative staff within the Department of Regenerative and Cancer Cell Biology at the Albany Medical College. This work was supported by start-up funds from the Albany Medical College.

AUTHOR CONTRIBUTIONS

J.S.L. conceived and designed the study. S.B.L. performed all experiments except for stiffness measurements on isolated nuclei treated with Dasatinib (performed by M.F.U.) and FRET assays (performed by J.S.L.). K.W.V. performed all flow cytometry and assisted with image analysis. J.S.L. wrote the manuscript with comments from all lab members.

COMPETING FINANCIAL INTERESTS

The authors declare no competing financial interests.

REFERENCES

1. Steeg, P.S. Targeting metastasis. *Nature reviews cancer* **16**, 201 (2016).
2. Yamada, K.M. & Sixt, M. Mechanisms of 3D cell migration. *Nature Reviews Molecular Cell Biology* **20**, 738-752 (2019).
3. Logue, J.S., Cartagena-Rivera, A.X. & Chadwick, R.S. c-Src activity is differentially required by cancer cell motility modes. *Oncogene* (2018).
4. Ullo, M.F. & Logue, J.S. Re-thinking preclinical models of cancer metastasis. *Oncoscience* **5**, 252-253 (2018).
5. Pandya, P., Orgaz, J.L. & Sanz-Moreno, V. Modes of invasion during tumour dissemination. *Mol Oncol* **11**, 5-27 (2017).

6. Paul, C.D., Mistriotis, P. & Konstantopoulos, K. Cancer cell motility: lessons from migration in confined spaces. *Nature Reviews Cancer* **17**, 131 (2017).

7. Liu, Y.J. *et al.* Confinement and low adhesion induce fast amoeboid migration of slow mesenchymal cells. *Cell* **160**, 659-672 (2015).

8. Logue, J.S. *et al.* Erk regulation of actin capping and bundling by Eps8 promotes cortex tension and leader bleb-based migration. *Elife* **4** (2015).

9. Charras, G.T., Yarrow, J.C., Horton, M.A., Mahadevan, L. & Mitchison, T.J. Non-equilibration of hydrostatic pressure in blebbing cells. *Nature* **435**, 365-369 (2005).

10. Ruprecht, V. *et al.* Cortical contractility triggers a stochastic switch to fast amoeboid cell motility. *Cell* **160**, 673-685 (2015).

11. Bergert, M. *et al.* Force transmission during adhesion-independent migration. *Nat Cell Biol* **17**, 524-529 (2015).

12. Venturini, V. *et al.* The nucleus measures shape deformation for cellular proprioception and regulates adaptive morphodynamics. *bioRxiv*, 865949 (2019).

13. Lomakin, A.J. *et al.* The nucleus acts as a ruler tailoring cell responses to spatial constraints. *bioRxiv*, 863514 (2019).

14. Wolf, K. *et al.* Physical limits of cell migration: control by ECM space and nuclear deformation and tuning by proteolysis and traction force. *J Cell Biol* **201**, 1069-1084 (2013).

15. Madsen, C.D. & Sahai, E. Cancer dissemination--lessons from leukocytes. *Dev Cell* **19**, 13-26 (2010).

16. Chow, K.-H., Factor, R.E. & Ullman, K.S. The nuclear envelope environment and its cancer connections. *Nature Reviews Cancer* **12**, 196 (2012).

17. Guilluy, C. *et al.* Isolated nuclei adapt to force and reveal a mechanotransduction pathway in the nucleus. *Nature cell biology* **16**, 376-381 (2014).

18. Tifft, K.E., Bradbury, K.A. & Wilson, K.L. Tyrosine phosphorylation of nuclear-membrane protein emerin by Src, Abl and other kinases. *Journal of cell science* **122**, 3780-3790 (2009).

19. Georgouli, M. *et al.* Regional Activation of Myosin II in Cancer Cells Drives Tumor Progression via a Secretory Cross-Talk with the Immune Microenvironment. *Cell* **176**, 757-774 e723 (2019).

20. Cantelli, G. *et al.* TGF-β-induced transcription sustains amoeboid melanoma migration and dissemination. *Current biology* **25**, 2899-2914 (2015).

21. Tozluoglu, M. *et al.* Matrix geometry determines optimal cancer cell migration strategy and modulates response to interventions. *Nat Cell Biol* **15**, 751-762 (2013).

22. Logue, J., Chadwick, R. & Waterman, C. A simple method for precisely controlling the confinement of cells in culture. (2018).

23. Lavenus, S.B., Tudor, S.M., Ullo, M.F., Vosatka, K.W. & Logue, J.S. A flexible network of vimentin intermediate filaments promotes migration of amoeboid cancer cells through confined environments. *J Biol Chem* **295**, 6700-6709 (2020).

24. Le, H.Q. *et al.* Mechanical regulation of transcription controls Polycomb-mediated gene silencing during lineage commitment. *Nature cell biology* **18**, 864 (2016).

25. Pfaff, J. *et al.* Emery–Dreifuss muscular dystrophy mutations impair TRC40-mediated targeting of emerin to the inner nuclear membrane. *J Cell Sci* **129**, 502-516 (2016).

26. Holaska, J.M., Kowalski, A.K. & Wilson, K.L. Emerin caps the pointed end of actin filaments: evidence for an actin cortical network at the nuclear inner membrane. *PLoS biology* **2**, e231 (2004).

27. Ouyang, M., Sun, J., Chien, S. & Wang, Y. Determination of hierarchical relationship of Src and Rac at subcellular locations with FRET biosensors. *Proc Natl Acad Sci U S A* **105**, 14353-14358 (2008).

28. Verveer, P.J., Rocks, O., Harpur, A.G. & Bastiaens, P.I. Measuring FRET by acceptor photobleaching. *CSH Protoc* **2006** (2006).

29. Ho, C.Y., Jaalouk, D.E., Vartiainen, M.K. & Lammerding, J. Lamin A/C and emerin regulate MKL1–SRF activity by modulating actin dynamics. *Nature* **497**, 507 (2013).

30. Neisch, A.L. & Fehon, R.G. Ezrin, Radixin and Moesin: key regulators of membrane-cortex interactions and signaling. *Curr Opin Cell Biol* **23**, 377-382 (2011).

31. Ross, T.D. *et al.* Integrins in mechanotransduction. *Curr Opin Cell Biol* **25**, 613-618 (2013).

32. Gorelik, R. & Gautreau, A. Quantitative and unbiased analysis of directional persistence in cell migration. *Nat Protoc* **9**, 1931-1943 (2014).

33. Meijering, E., Dzyubachyk, O. & Smal, I. Methods for cell and particle tracking. *Methods Enzymol* **504**, 183-200 (2012).

FIGURES

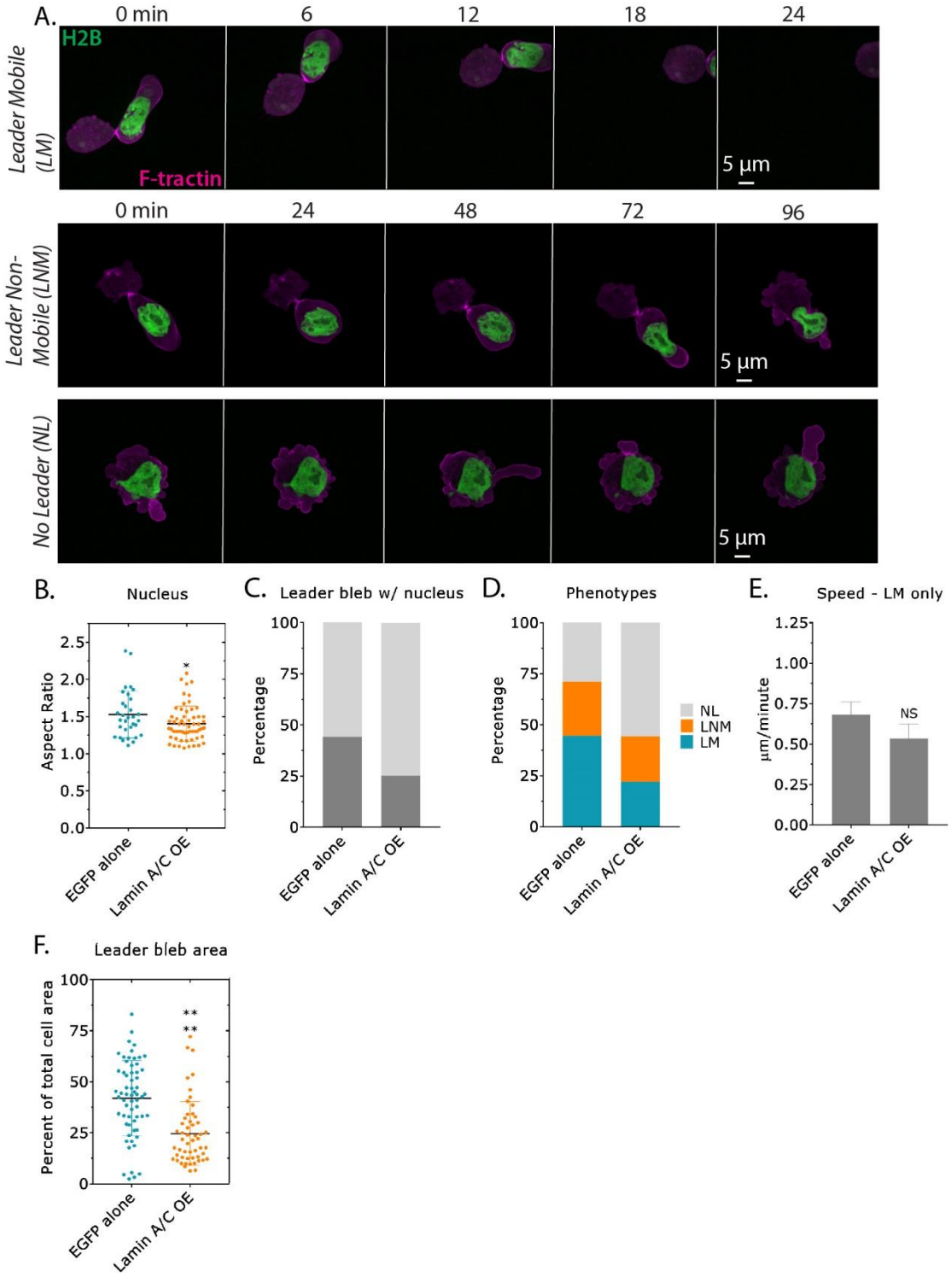

Figure 1. Confined (leader bleb-based) migration is regulated by nuclear stiffness. A. Time-lapse imaging of melanoma A375-M2 cells transiently transfected with H2B-mEmerald and F-traction-FusionRed to mark nuclei and F-actin, respectively, confined using the PDMS slab-based approach (~3 μm beads). **B.** Nuclear aspect ratio for cells over-expressing EGFP alone or Lamin A/C-mEmerald (mean +/- SD; two-tailed Student's t-test). **C.** Percent cells with leader blebs containing the nucleus for EGFP alone (39/73 cells) or Lamin A/C-mEmerald (21/70 cells). **D.** Percent NL, LNM, and LM for cells over-expressing EGFP alone or Lamin A/C-mEmerald. Statistical significance was determined using a Chi-squared test ($\chi^2=1.16 \times 10^{-8}$). **E.** Instantaneous speeds for leader mobile (LM) cells over-expressing EGFP alone or Lamin A/C-mEmerald (mean +/- SEM; two-tailed Student's t-test). **F.** Leader bleb area (calculated as the percent of total cell area) for cells over-expressing EGFP alone or Lamin A/C-mEmerald (mean +/- SD; two-tailed Student t-test). See also supplemental figure 1 and movies 1-3. All data are representative of at least three independent experiments. * - $p \leq 0.05$, ** - $p \leq 0.01$, *** - $p \leq 0.001$, and **** - $p \leq 0.0001$

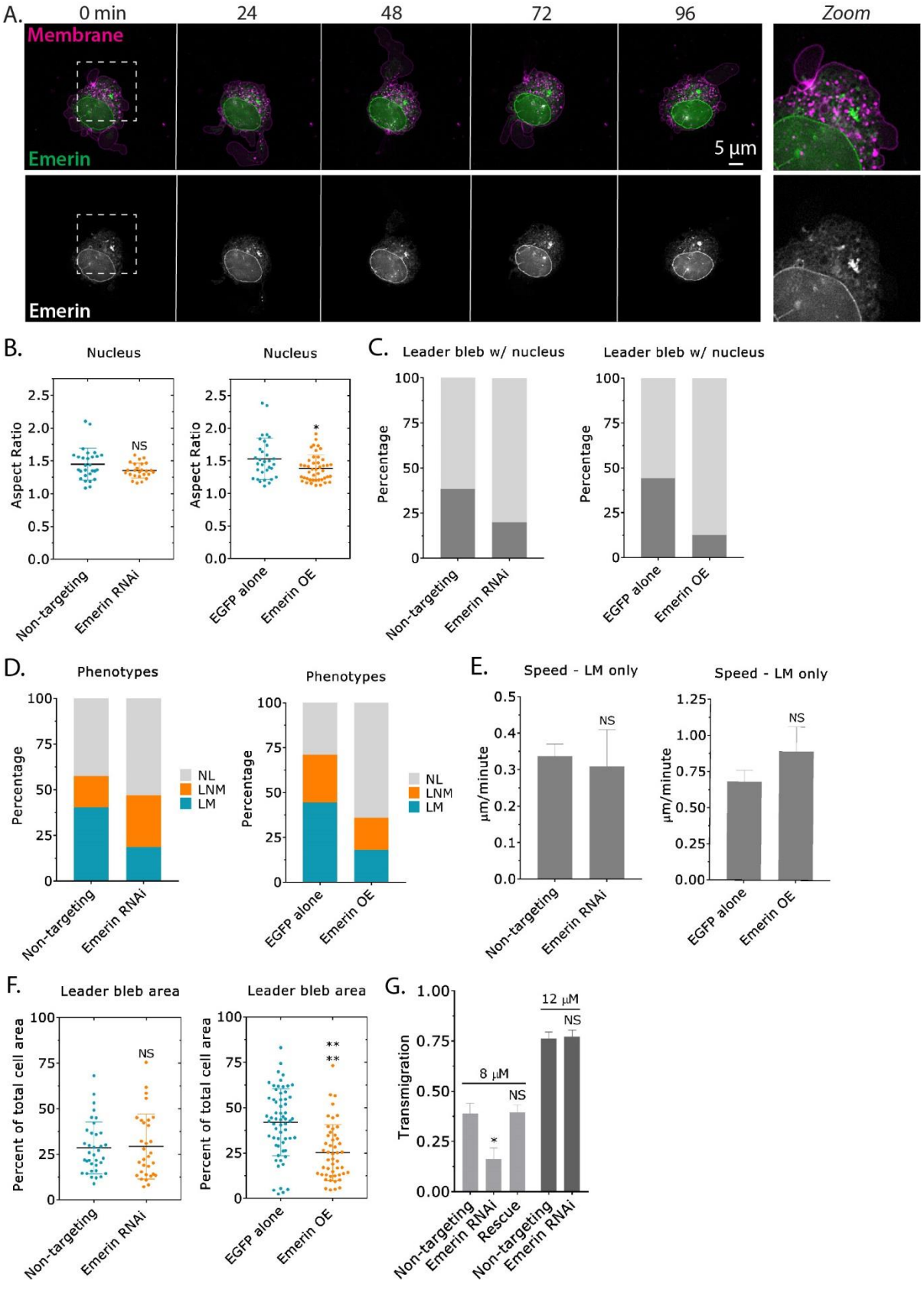

Figure 2. Endogenous levels of emerin promote confined migration. A. Time-lapse imaging of a melanoma A375-M2 cell over-expressing EGFP-emerin, membrane dye (far-red fluorescent), and confined using the PDMS slab-based approach (~3 μm beads). Zoom shows emerin predominantly at the nuclear envelope. **B.** Nuclear aspect ratio of emerin RNAi (left) and over-expressing (right) cells (mean +/- SD; two-tailed Student's t-test). **C.** Percent cells with leader blebs containing the nucleus for non-targeting (20/43 cells; left), emerin RNAi (7/32 cells; left), EGFP alone (39/73 cells; right), and EGFP-emerin (8/50 cells; right). **D.** Percent NL, LNM, and LM for emerin RNAi (left) and over-expressing (right) cells. Statistical significance was determined using a Chi-squared test (emerin RNAi; $\chi^2=2.97 \times 10^{-7}$, over-expression; $\chi^2=7.69 \times 10^{-14}$). **E.** Instantaneous speeds for leader mobile (LM) cells after emerin RNAi (left) and over-expression (right) (mean +/- SEM; two-tailed Student's t-test). **F.** Leader bleb area (calculated as the percent of total cell area) for cells after emerin RNAi (left) and over-expression (right) (mean +/- SD; two-tailed Student's t-test). **G.** *Left,* transmigration through 8 μm pores after emerin RNAi and rescue (mean +/- SEM; multiple-comparison test post-hoc). *Right,* transmigration through 12 μm pores after emerin RNAi (mean +/- SEM; two-tailed Student's t-test). See also supplemental movie 4. All data are representative of at least three independent experiments. * - $p \leq 0.05$, ** - $p \leq 0.01$, *** - $p \leq 0.001$, and **** - $p \leq 0.0001$

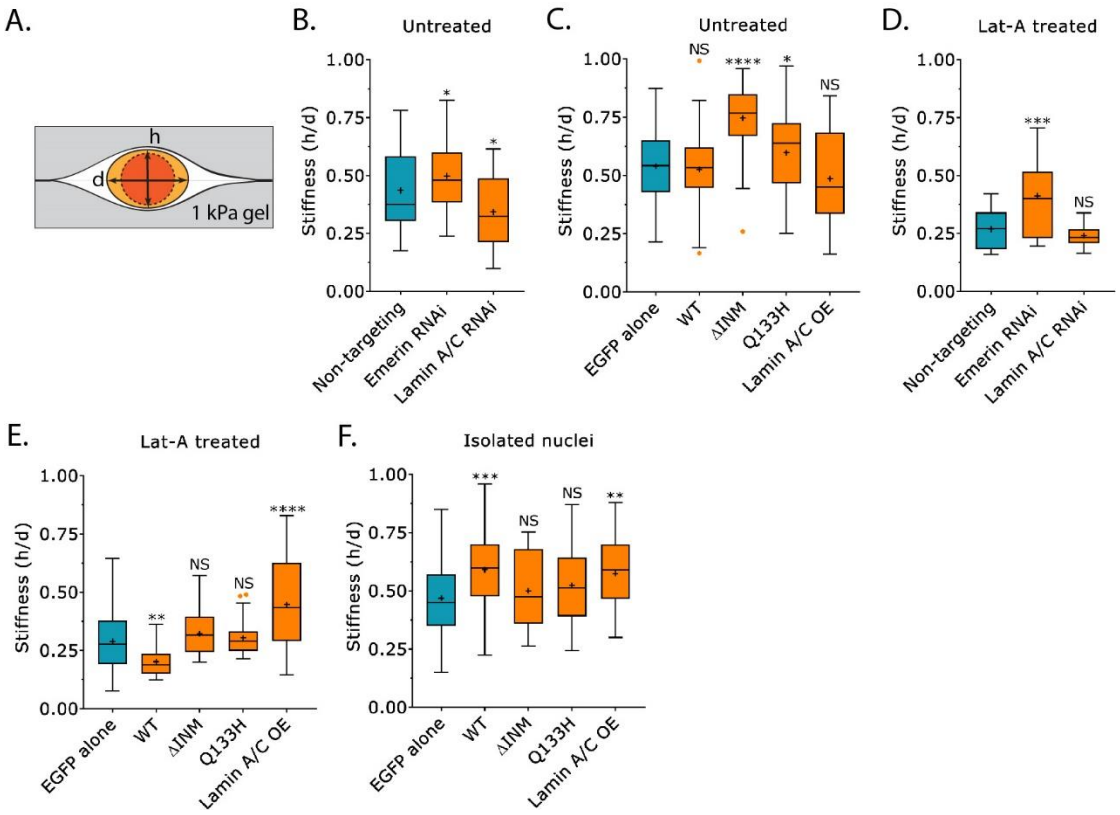

Figure 3. Nuclear stiffness is precisely regulated by emerin. **A.** Schematic representation of the 'gel sandwich approach' for measuring stiffness. **B.** Stiffness (*h*/*d*) for intact (untreated) cells after non-targeting (53 cells), emerin (49 cells), or Lamin A/C RNAi (33 cells) ("+" and line denote the mean and median, respectively; multiple-comparison test post-hoc). **C.** Stiffness (*h*/*d*) for intact (untreated) cells over-expressing EGFP alone (169 cells), emerin WT (69 cells), ΔINM (66 cells), Q133H (105 cells), and Lamin A/C (29 cells) ("+" and line denote the mean and median, respectively; multiple-comparison test post-hoc). **D.** Stiffness (*h/d*) for Latrunculin-A (Lat-A; 500 nM) treated cells after non-targeting (13 cells), emerin 15 cells), or Lamin A/C RNAi (30 cells) ("+" and line denote the mean and median, respectively; multiple-comparison test post-hoc). **E.** Stiffness (*h/d*) for Lat-A (500 nM) treated cells over-expressing EGFP alone (105 cells), emerin WT (28 cells), ΔINM (35 cells), Q133H (41 cells), and Lamin A/C (20 cells) ("+" and line denote the mean and median, respectively; multiple-comparison test post-hoc). **F.** Stiffness (*h/d*) for isolated nuclei (post cell fractionation) after over-expressing EGFP alone (81

nuclei), emerin WT (45 nuclei), ΔINM (23 nuclei), Q133H (41 nuclei), and Lamin A/C (35 nuclei). See also supplemental figures S2-3. All data are representative of at least three independent experiments. * - $p \leq 0.05$, ** - $p \leq 0.01$, *** - $p \leq 0.001$, and **** - $p \leq 0.0001$

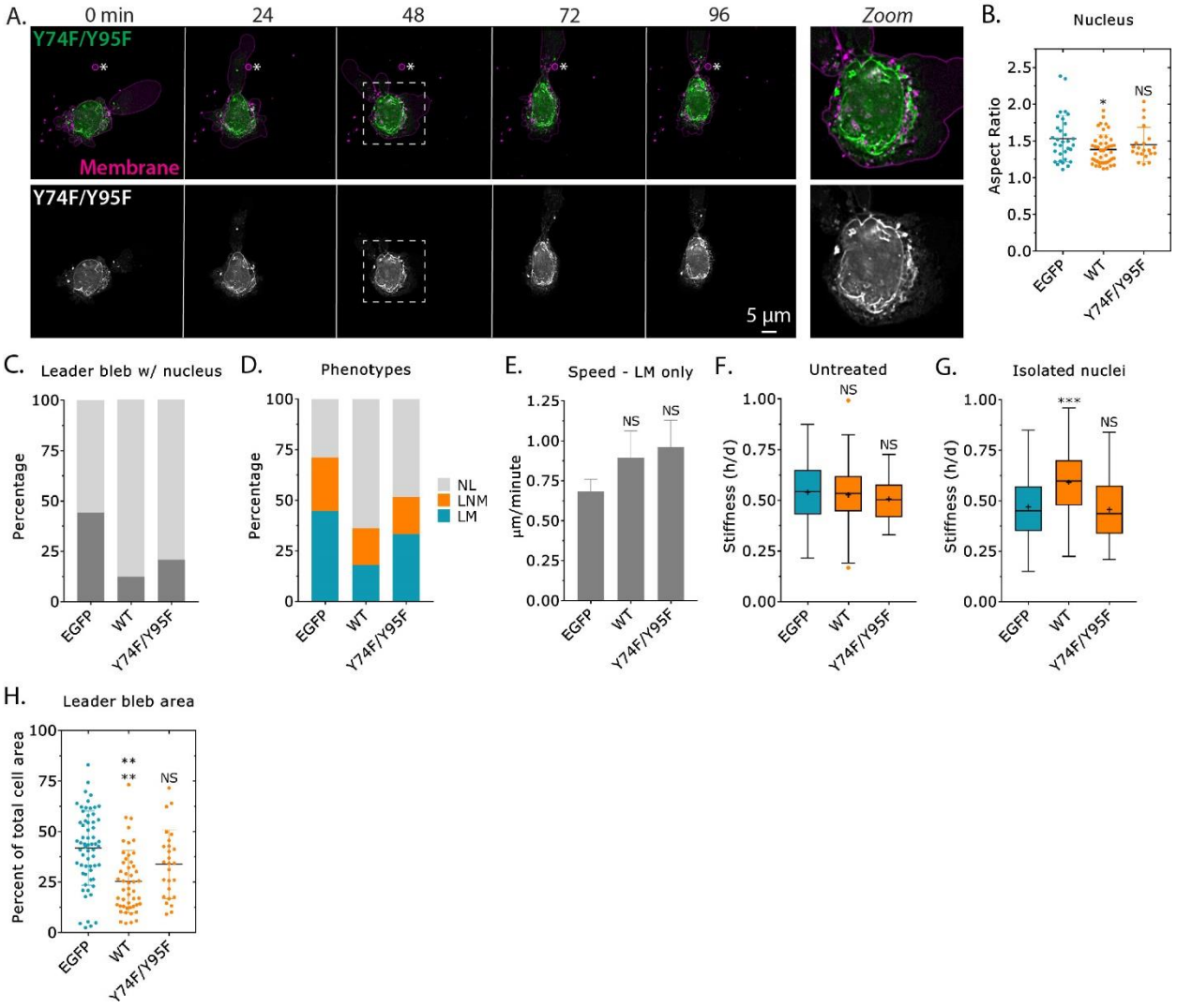

Figure 4. Confined (leader bleb-based) migration is insensitive to increasing levels of non-phosphorylatable (Y74F/Y95F) emerin. **A.** Time-lapse imaging of a melanoma A375-M2 cell over-expressing non-phosphorylatable (Y74F/Y95F; N-terminal EGFP) emerin, membrane dye (far-red fluorescent), and confined using the PDMS slab-based approach (~3 µm beads). Zoom shows emerin (Y74F/Y95F) predominantly at the nuclear envelope. **B.** Nuclear aspect ratio of cells over-expressing EGFP alone, emerin WT, and Y74F/Y95F (mean +/- SD; multiple-comparison test post-hoc). **C.** Percent cells with leader blebs containing the nucleus for EGFP alone (39/73 cells), emerin WT (8/50 cells), and Y74F/Y95F (7/33 cells). **D.** Percent NL, LNM, and LM for EGFP alone, emerin WT, and Y74F/Y95F. Statistical significance was determined

using a Chi-squared test (EGFP alone vs. Y74F/Y95F; χ^2=0.000104). **E.** Instantaneous speeds for cells over-expressing EGFP alone, emerin WT, and Y74F/Y95F (mean +/- SEM; multiple-comparison test post-hoc). **F.** Stiffness (*h/d*) of intact (untreated) cells over-expressing EGFP alone (169 cells), emerin WT (69 cells), and Y74F/Y95F (57 cells) ("+" and line denote the mean and median, respectively; multiple-comparison test post-hoc). **G.** Stiffness (*h/d*) of isolated nuclei (post cell fractionation) after over-expressing EGFP alone (81 nuclei), emerin WT (45 nuclei), and Y74F/Y95F (42 nuclei) ("+" and line denote the mean and median, respectively; multiple-comparison test post-hoc). **H.** Leader bleb area (calculated as the percent of total cell area) for cells over-expressing EGFP alone, emerin WT, and Y95F/Y74F (mean +/- SD; multiple-comparison test post-hoc). See also supplemental movie 5. All data are representative of at least three independent experiments. * - $p \leq 0.05$, ** - $p \leq 0.01$, *** - $p \leq 0.001$, and **** - $p \leq 0.0001$

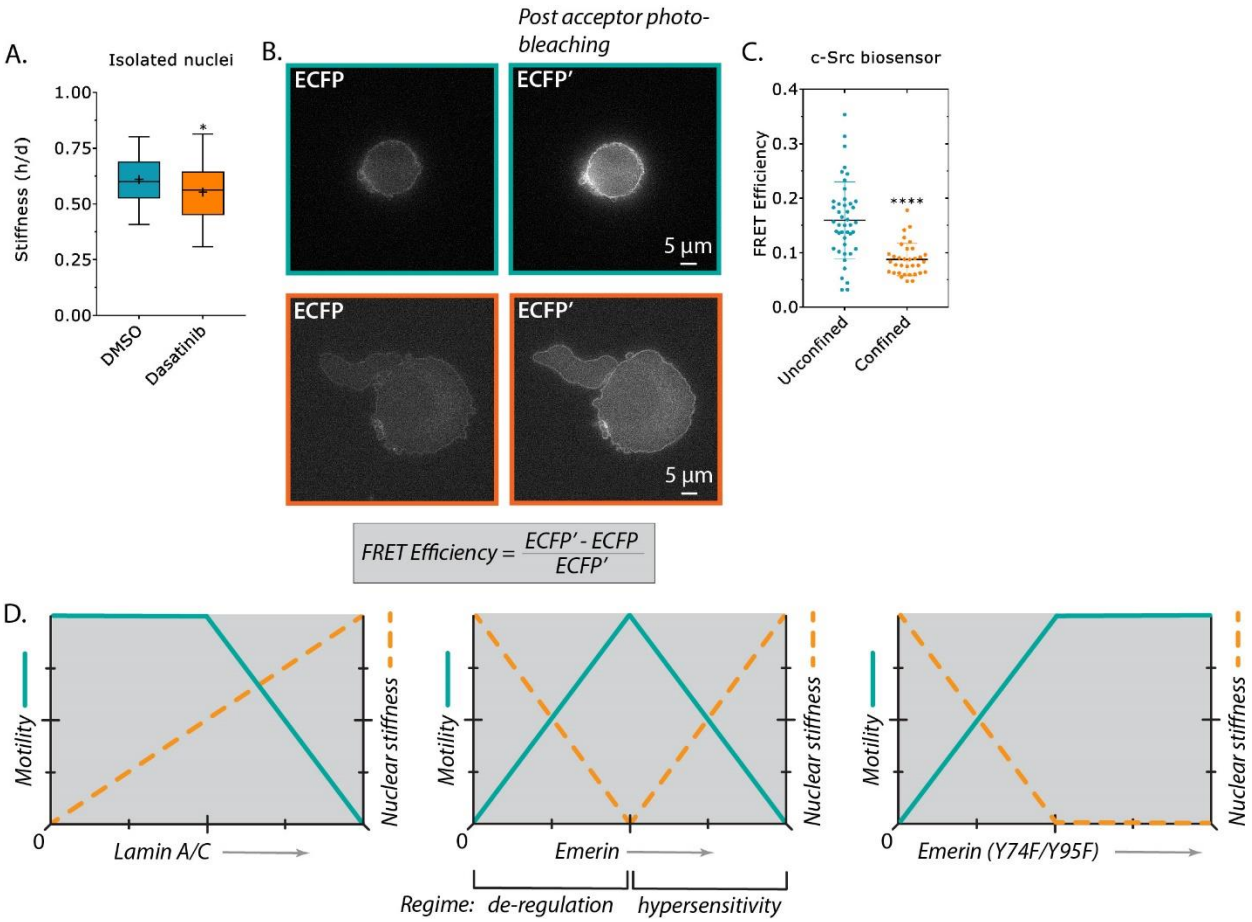

Figure 5. Src activity in unconfined vs. confined cells. **A.** Stiffness (*h/d*) of isolated nuclei treated with DMSO (53 nuclei) or the Src inhibitor, Dasatinib (500 nM; post cell fractionation) (56 nuclei) ("+" and line denote the mean and median, respectively; two-tailed Student's t-test). **B.** *Top*, ECFP (before photobleaching; FRET acceptor from Src biosensor) and ECFP' (after photobleaching; FRET acceptor from Src biosensor) from unconfined cells, which were freshly plated on uncoated glass. *Bottom*, ECFP (before photobleaching; FRET acceptor from Src biosensor) and ECFP' (after photobleaching; FRET acceptor from Src biosensor) from confined cells, which were confined using the PDMS slab-based approach (~ 3 µm beads). Equation for calculating FRET efficiency is shown. **C.** Quantitative evaluation of FRET efficiency for unconfined vs. confined cells (mean +/- SD; two-tailed Student's t-test). **D.** Qualitative relationship between motility (confined) and nuclear stiffness as a function of increasing levels

of Lamin A/C (left), emerin (middle), or emerin (Y74F/Y95F; right). All data are representative of at least three independent experiments. * - $p \leq 0.05$, ** - $p \leq 0.01$, *** - $p \leq 0.001$, and **** - $p \leq 0.0001$

SUPPLEMENTAL FIGURES

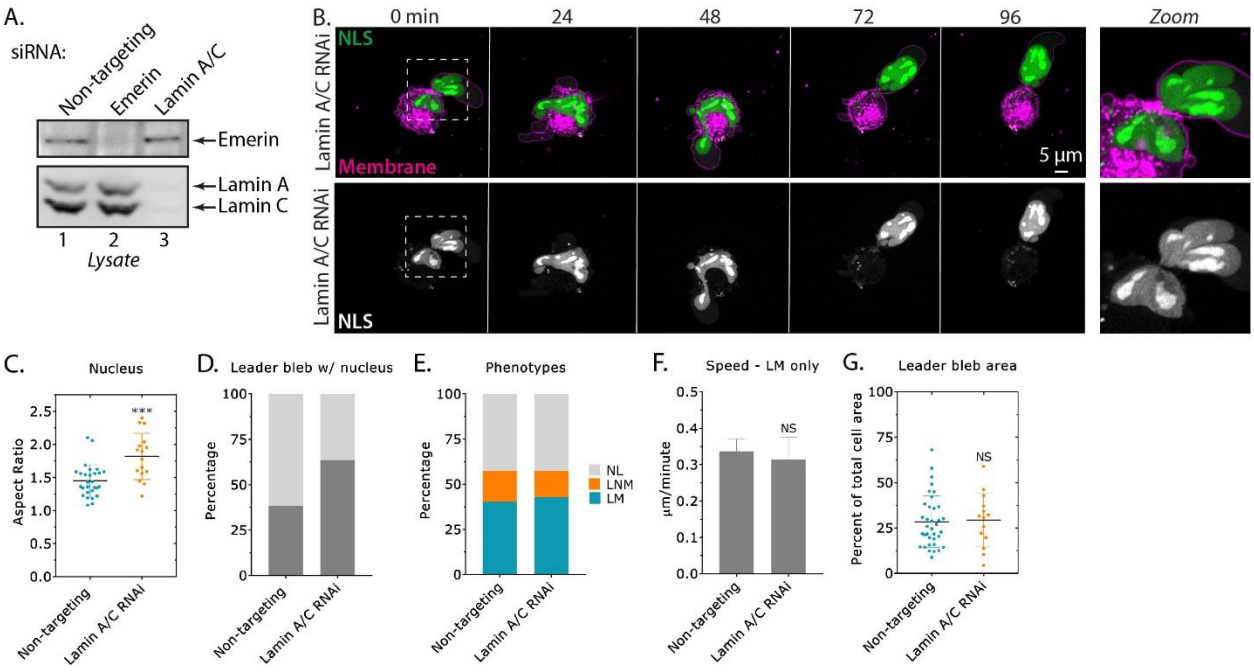

Supplemental figure 1. A. Western blot confirmation of emerin and Lamin A/C RNAi in melanoma A375-M2 cells. Cells were treated for 5 days with each Locked Nucleic Acid (LNA; 50 nM) to achieve a near complete removal of each protein. **B.** Time-lapse imaging of a melanoma A375-M2 cell after Lamin A/C RNAi with Nuclear Localization Sequence (NLS) tagged mEmerald, membrane dye (far-red fluorescent), and confined using our PDMS slab-based approach (~3 µm beads). Zoom shows the extent of nuclear deformation in Lamin A/C RNAi cells. **C.** Nuclear aspect ratio for cells after Lamin A/C RNAi (mean +/- SD; two-tailed Student's t-test). **D.** Percent cells with leader blebs containing the nucleus for non-targeting (20/43 cells) and Lamin A/C RNAi (12/21 cells). **E.** Percent NL, LNM, and LM for Lamin A/C RNAi cells. Statistical significance was determined using a Chi-squared test (χ^2=0.748). **F.** Instantaneous speeds for leader mobile (LM) cells after Lamin A/C RNAi (mean +/- SEM; two-tailed Student's t-test). **G.** Leader bleb area (calculated as the percent of total cell area) for cells after Lamin A/C RNAi (mean +/- SD; two-tailed Student's t-test). All data are representative of

at least three independent experiments. * - $p \leq 0.05$, ** - $p \leq 0.01$, *** - $p \leq 0.001$, and **** - $p \leq 0.0001$

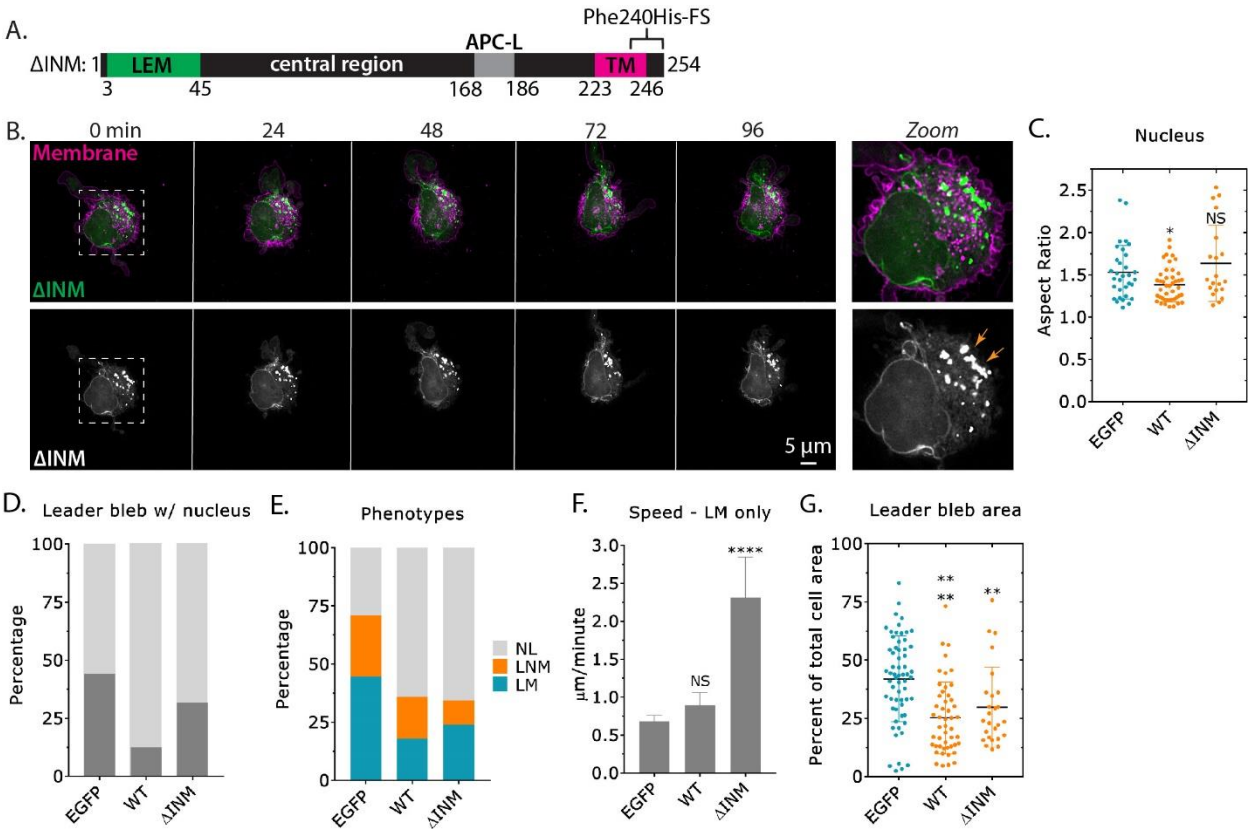

Supplemental figure 2. **A.** Cartoon of the frame shift mutation, Phe240His-FS, near the transmembrane (TM) domain for retaining emerin within the ONM/ER (termed ΔINM). LEM (Lap2, emerin, MAN1) domain and APC-like (APC-L) domain. **B.** Time-lapse imaging of a melanoma A375-M2 cell with EGFP-emerin (ΔINM), membrane dye (far-red dye), and confined using the PDMS slab-based approach (~3 μm beads). Zoom shows emerin (ΔINM) predominantly at the ONM/ER. **C.** Nuclear aspect ratio of cells over-expressing EGFP alone, emerin WT, and ΔINM (mean +/- SD; multiple-comparison test post-hoc). **D.** Percent cells with leader blebs containing the nucleus for EGFP alone (39/73 cells), emerin WT (8/50 cells), and ΔINM (8/28 cells). **E.** Percent NL, LNM, and LM for EGFP alone, emerin WT, and ΔINM. Statistical significance was determined using a Chi-squared test (EGFP alone vs. ΔINM; $\chi^2=2.42 \times 10^{-15}$). **F.** Instantaneous speeds for leader mobile (LM) cells over-expressing EGFP alone, emerin WT, and ΔINM (mean +/- SEM; multiple-comparison test post-hoc). **G.** Leader bleb area (calculated as the percent of total cell area) for cells over-expressing EGFP alone,

emerin WT, and ΔINM (mean +/- SD; multiple-comparison test post-hoc). See also figure 3. All data are representative of at least three independent experiments. * - $p \leq 0.05$, ** - $p \leq 0.01$, *** - $p \leq 0.001$, and **** - $p \leq 0.0001$

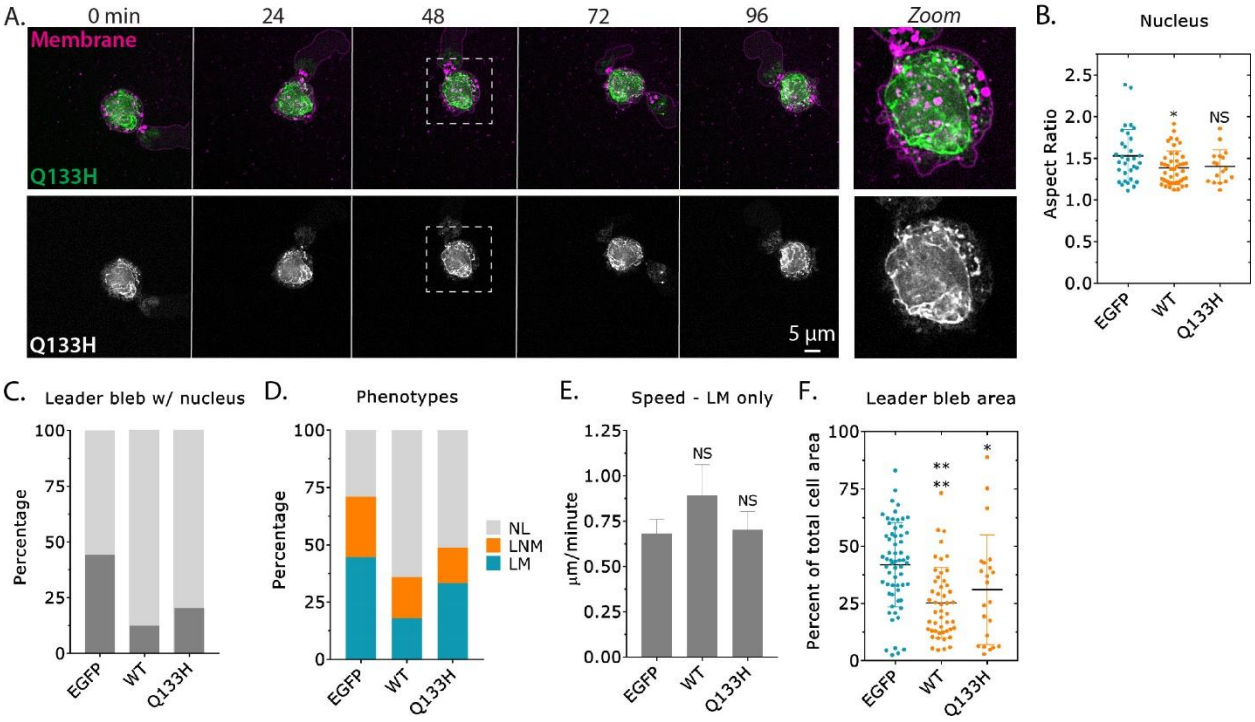

Supplemental figure 3. **A.** Time-lapse imaging of a melanoma A375-M2 cell with EGFP-emerin (Q133H), membrane dye (far-red fluorescent), and confined using the PDMS slab-based approach (~3 µm beads). Zoom shows emerin (Q133H) predominantly at the nuclear envelope. **B.** Nuclear aspect ratio for cells over-expressing EGFP alone, emerin WT, and Q133H (mean +/- SD; multiple-comparison test post-hoc). **C.** Percent cells with leader blebs containing the nucleus for EGFP alone (39/73 cells), emerin WT (8/50 cells), and Q133H (9/34 cells). **D.** Percent NL, LNM, and LM for EGFP alone, emerin WT, and Q133H. Statistical significance was determined using a Chi-squared test (EGFP alone vs. Q133H; $\chi^2=5.07 \times 10^{-6}$). **E.** Instantaneous speeds for leader mobile (LM) cells over-expressing EGFP alone, emerin WT, and Q133H (mean +/- SEM; multiple-comparison test post-hoc). **F.** Leader bleb area (calculated as the percent of total cell area) for cells over-expressing EGFP alone, emerin WT, and Q133H (mean +/- SD; multiple-comparison test post-hoc). See also figure 3. All data are representative of at least three independent experiments. * - $p \leq 0.05$, ** - $p \leq 0.01$, *** - $p \leq 0.001$, and **** - $p \leq 0.0001$

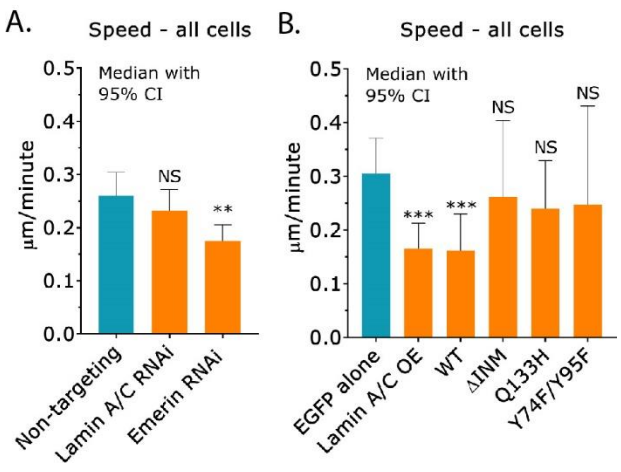

Supplemental figure 4. **A.** Instantaneous speeds for all cells (LM + LNM + NL) after Lamin A/C or emerin RNAi (median +/- 95% CI; multiple-comparison test post-hoc). **B.** Instantaneous speeds for all cells (LM + LNM + NL) over-expressing EGFP alone, Lamin A/C, emerin WT, ΔINM, Q133H, and Y74F/Y95F (median +/- 95% CI; multiple-comparison test post-hoc). All data are representative of at least three independent experiments. * - $p \leq 0.05$, ** - $p \leq 0.01$, *** - $p \leq 0.001$, and **** - $p \leq 0.0001$

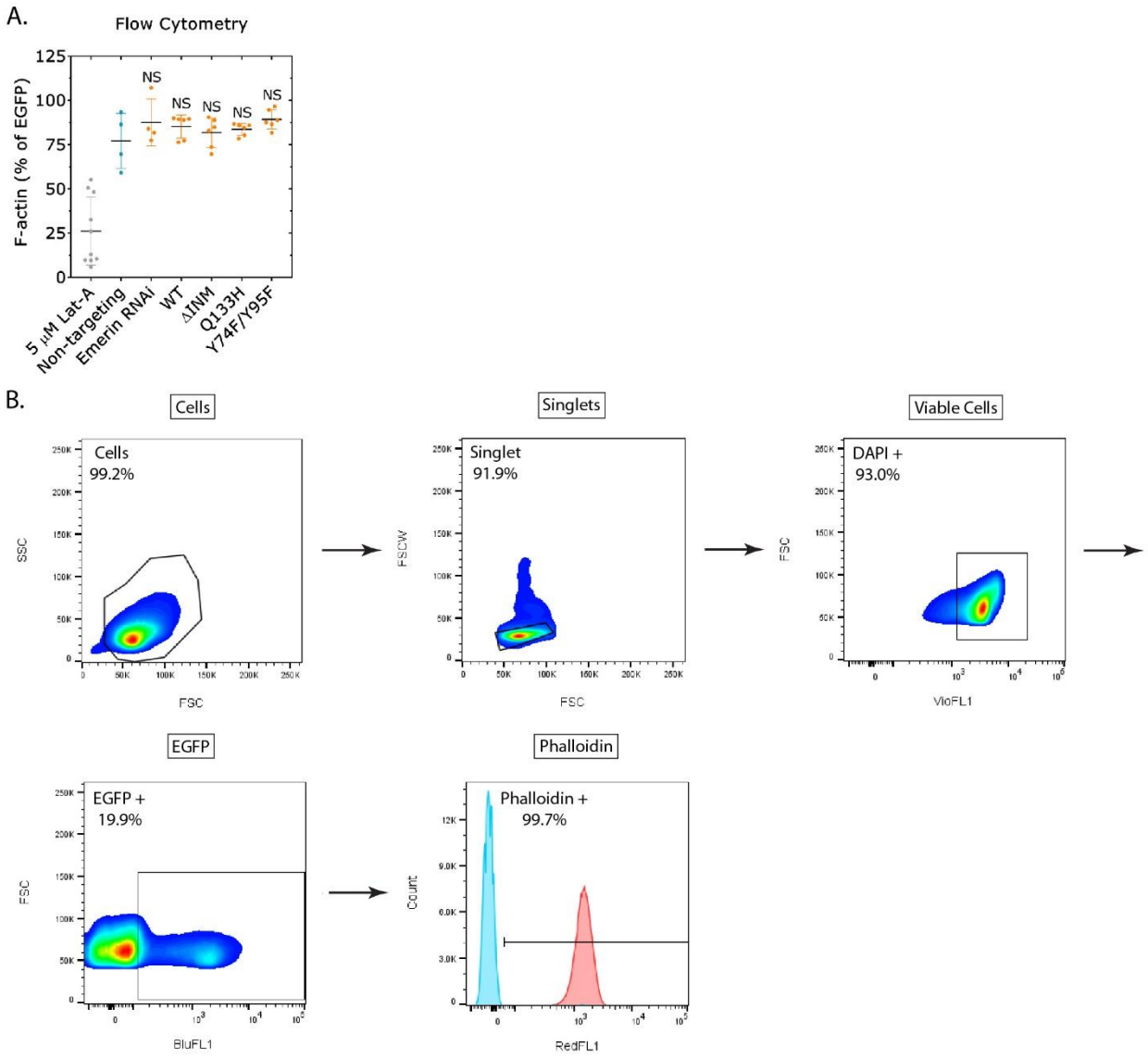

Supplemental figure 5. **A.** Flow cytometry analysis of total F-actin, as measured by phalloidin (far-red fluorescent) binding in cells treated with Latrunculin-A (Lat-A; 5 µM), non-targeting, emerin RNAi, over-expressing emerin WT, ΔINM, Q133H, and Y74F/Y95F (relative to cells over-expressing EGFP alone) (mean +/- SD; multiple-comparison test post-hoc). Each point corresponds to a Median Fluorescence Intensity (MFI). **B.** Flow gating strategy. Cells are isolated based on instrument calibration. Single cells were isolated by comparing forward scatter width and height. Viable cells were identified using DAPI staining while EGFP fluorescence was used to identify transfected cells. Cells that were positively stained with

phalloidin (red curve) were isolated based on a gate created referencing unstained cells (blue curve) for analysis. * - $p \leq 0.05$, ** - $p \leq 0.01$, *** - $p \leq 0.001$, and **** - $p \leq 0.0001$

SUPPLEMENTAL MOVIES

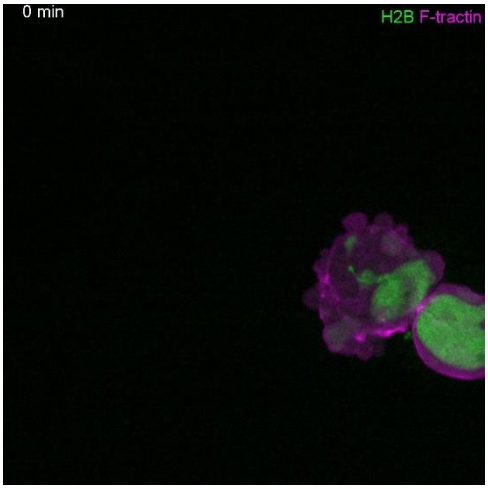

Supplemental movie 1. Time-lapse imaging of a leader mobile (LM) cell under PDMS transiently expressing H2B-mEmerald and F-tractin-FusionRed.

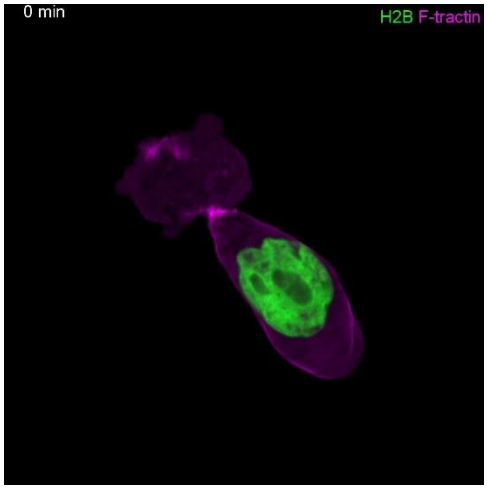

Supplemental movie 2. Time-lapse imaging of a leader non-mobile (LNM) cell under PDMS transiently expressing H2B-mEmerald and F-tractin-FusionRed.

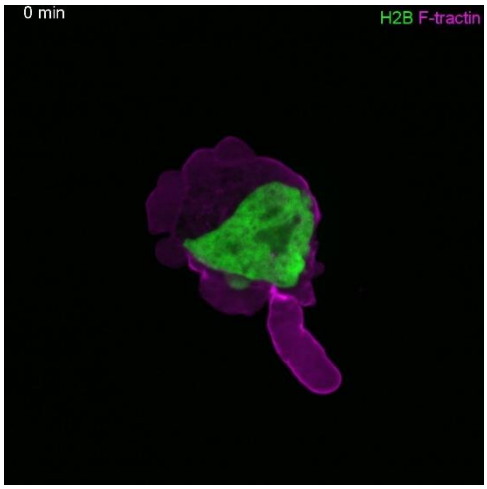

Supplemental movie 3. Time-lapse imaging of a no leader (NL) cell under PDMS transiently expressing H2B-mEmerald and F-tractin-FusionRed.

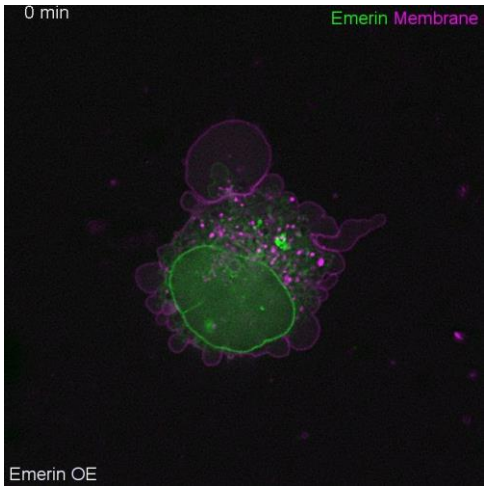

Supplemental movie 4. Time-lapse imaging of an A375-M2 cell over-expressing EGFP-emerin, membrane dye (far-red fluorescent), and confined using the PDMS slab-based approach (~3 µm beads).

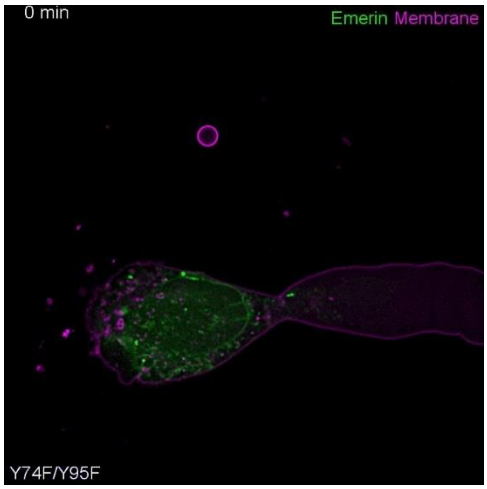

Supplemental movie 5. Time-lapse imaging of an A375-M2 cells over-expressing EGFP-emerin (Y74F/Y95F), membrane dye (far-red fluorescent), and confined using the PDMS slab-based approach (~3 µm beads).